STUDIA UNIVERSITATIS BABES-BOLYAI, PHYSICA, LIV, 1, 2009

FINITE DIFFERENCE TIME DOMAIN (FDTD) CALCULATIONS OF SURFACE PLASMON RESONANCE OF DIFFERENT SIZE AND SHAPE METALLIC NANOPARTICLES

FRANÇOIS K. GUEDJE[1,*], SANDA BOCA[1], MONICA POTARA[1], ARINA MODREA[2], SIMION ASTILEAN[1]

ABSTRACT. In this work we employ the Finite Difference Time Domain (FDTD) method to calculate the optical spectra and the intensity of local electromagnetic field at the surface of different size, shape and assembling configuration of nanoparticles (NPs) with a view to optimize their sensing activity. We first consider gold nanospheres of 20 nm diameter where analytical solutions are available for comparison. The other shapes we consider include gold nanorods and silver nanoprisms which are particularly important for applications, because they allow tuning the plasmon resonances across the whole visible and near infrared range. The theoretical spectra are compared with experimental data from synthesized samples in our laboratory.

Keywords: nanoparticle, plasmonics, FDTD.

1. Introduction

In recent years, plasmonics has attracted a great deal of attention due to its important potential toward applications in sensing, medical imaging and information processing [1]. This branch of photonics develops new concepts to confine light beyond the diffraction limit and enhance the electromagnetic field at the nanoscale. The past decade has seen significant advances in the synthesis and fabrication of disperse noble metal nanoparticles with a variety of shapes, from spheres to branched multipods. These particles are studied for a large variety of applications due to their localized surface plasmon resonance (LSPR). LSPR occurs when the electromagnetic field of light drives the collective oscillations of a nanoparticle's free electrons into resonance.

[*] On leave from the International Chair in Mathematical Physics and Applications, Université d'Abomey-Calavi, 01 BP 526 Cotonou, Bénin

[1] Babes-Bolyai University, Faculty of Physics and Institute for Interdisciplinary Experimental Research, Nanobiophotonics Center, Treboniu Laurian Street 42, 400271 Cluj-Napoca, Romania

[2] Petru Maior University, Faculty of Engineering, Tirgu-Mures, Romania

The LSPR enables many relevant applications including biological and chemical sensing [2-3], biological imaging labels [4], and nanoscale optical waveguides [5]. In particular, LSPR in the near-infrared (NIR) enables a significant step toward diagnostic and therapeutic in cancer research and other biomedical applications [6].

Here we employ the FDTD method to evaluate the plasmonic resonances and the intensity of local electromagnetic field at the surface of different size, shape and assembling configuration of GNPs in view of optimizing their sensor sensitivity. We first consider gold nanospheres, and we compare the results with available analytical solutions. Then we consider the nanorods with variable aspect ratio. For other particles of sufficiently anisotropy, like the case of nanoprism, it can give rise to additional peaks in the absorption spectrum as a result of multipolar plasmon excitation. In most of the works dedicated to investigating metallic nanostructures the background is usually air. In this work, we study the optical properties of the nanostructure within a natural surrounding medium different from air. This allowed to explain and better understand the effect of layers of cetyltrimethyl ammonium bromide (CTAB) surfactant and methoxy polyethylene glycol-thiol (mPEG-SH) in case of gold nanorods and chitosan polymers in case of silver nanoparticles.

2. Numerical Methodology

Mie [7] was the first who solved exactly and completely the problem of plane electromagnetic wave scattering by a homogeneous dielectric sphere. To properly treat the interaction of nanoparticles with optical fields, a full electromagnetic solution to the Maxwell's equation is needed. For more complex geometries, one has to rely on numerical simulations. Several methods for numerically solving electromagnetism for arbitrary geometry exist. Of all, the finite difference time domain (FDTD) technique of Taflove [9] and Sullivan [10] has proved to be a powerful tool to calculate the spectra as well as the near field properties of metal colloids.

This method solves the time-dependent Maxwell's equations by discretizing space and time and involves a relativity simple time-stepping algorithm. The electric flux dependent form of Maxwell's equations is given by:

$$\frac{\partial \vec{D}}{\partial t} = \nabla \times \vec{H} \tag{1}$$

$$D(\omega) = \varepsilon(\omega)\, E(\omega) \tag{2}$$

$$\frac{\partial \vec{H}}{\partial t} = -\frac{1}{\mu_0} \nabla \times \vec{E} \tag{3}$$

Where $\vec{H}$, $\vec{E}$, and $\vec{D}$ are the magnetic, electric, and displacement field, respectively. μ_0 is the permeability of free space and $\varepsilon(\omega)$ the complex dielectric constant.

The technique consists of solving these equations on a discrete grid, replacing all derivatives with finite differences. Following the Yee algorithm [11], both $\vec{D}$ and $\vec{H}$ are offset in both space and time. This allows one to use central differences, making the algorithm second-order accurate. In one dimension, Equation (1) can be written as:

$$\frac{D^{n+1/2}(k) - D^{n-1/2}(k)}{\Delta t} = \frac{H^{n}(k+1/2) - H^{n}(k-1/2)}{\Delta x} \tag{4}$$

Where k is the spatial coordinate and the superscript n denotes time. It is then straightforward to solve for $D^{n+1/2}(k)$ in terms of $D^{n-1/2}(k)$, $H^{n}(k+1/2)$ and $H^{n}(k-1/2)$ which are already stored in memory. Two points must be taken into account. First, the grid Δu must be fine enough to describe the smallest spatial features, whether it is the particle geometry or particle separation, where u is the side of a cubical cell. The time step Δt must be chosen with even greater consideration. The FDTD algorithm is stable only if the condition $\Delta t \le \frac{\Delta u}{c\sqrt{3}}$ is verified. The simulation is generally computationally intensive when high spatial precision is required.

Typically, FDTD calculations have been carried out for dielectric materials. Recent advances have extended the use of FDTD to the treatment of the materials with frequency dependent, complex dielectric constants [12]. It is the category of real metals.

If the metal is assumed to follow the Drude model, one can write the permittivity ε as

$$\varepsilon(\omega) = \varepsilon_{\infty} - \frac{\omega_p^2}{\omega^2 + i\nu_c\omega} \tag{5}$$

Where ω is the angular frequency, ω_p is the plasma frequency, ν_c is the collision frequency and ε_{∞} the high frequency dielectric constant. The Drude model is appealing in that it is derived from the simplest physical picture of free electron gas. The response of near-field probe has been simulated [13] under Drude model using FDTD. However, the Drude model does not accurately describe the real and imaginary indices of refraction of noble metals over a wide frequency range. Also, the Fourier transform of the susceptibility is often not numerically stable.

3. Computation of optical spectra and field enhancements for nanoparticles of different shapes

Figure 1 shows the nanostructures we study using the code from Lumerical™ [14] and compare their theoretical spectra with experimental data from synthesized samples in our laboratory. All our results refer to absorption spectra

and field enhancement of gold nanosphere (diameter 20nm), gold nanorod (diameter 24nm, length 53nm), and regular silver nanoprisms (edge length of 100nm with variable thickness) in water solution.

Figure 1. Example of nanoparticles shapes (sphere, rod, and prism) we study in this work.

3.1 Gold nanosphere

In a first step, we calculate here the absorption for gold nanosphere by using FDTD method and compare our result with that given from the Mie theory [7, 15]. Figure 2a shows for comparison, the experimental data obtained in our laboratory, our result and Mie Theory, for gold nanosphere of diameter 27 nm in water. Figure 2b present the field enhancement at the Plasmon resonance (523.6nm). It shows the amplitude of the local charge density oscillation for the sphere. From the symmetries of the distribution, the resonance peak can be labeled as the dipole resonance.

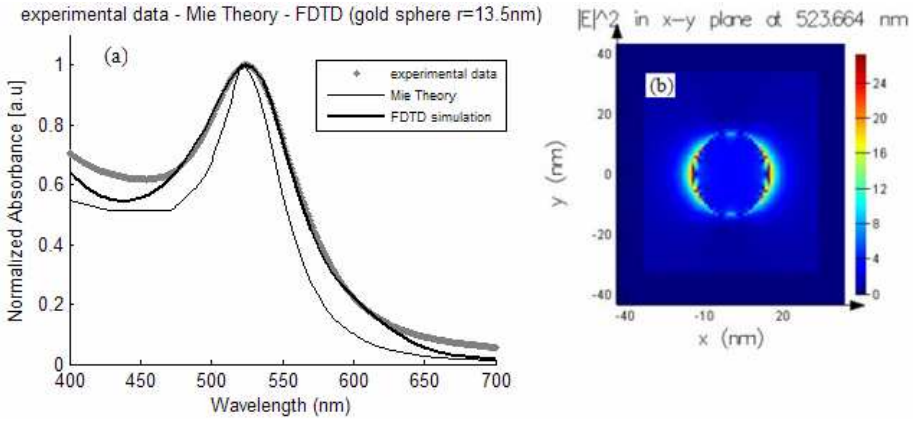

Figure 2. (a) The absorption spectra of a gold sphere with r =13.5nm radius calculated by FDTD and Mie theory. The experimental absorption spectrum is shown with dots for comparison. (b) The field enhancement ($|E^2|$) at the surface of nanoparticles calculated by FDTD. The field polarization is along x axis. The grid is 0.5 nm.

For gold dimers or particle chains, the spectra change drastically with the interparticle distance. We present in Figure 3 the results of the FDTD calculations. For the interparticle distance $d > D$, D being the sphere diameter, the electromagnetic coupling is very weak and the spectrum calculated for such a dimer coincides with

that of an isolated particle. It can be seen from Figure 3a that the transverse and longitudinal local surface resonances appear at shorter and longer wavelengths for $d << D$ when the electromagnetic coupling between particles is strong. When the spheres are in contact, the resonance splits into two distinct peaks. The first is the transversal resonance and the second is the longitudinal resonance for the dimer illuminated with incident plane wave. The longitudinal LSPR at 632 nm is not due to dipolar (521nm) but due to higher-polar collective oscillation of conduction electrons. Figures 3b show that the electromagnetic field at the junction excited by the light polarized along x-axis is larger than that excited by light polarized along y-axis. One can conclude that the SERS enhancement by longitudinal LSPs is due to the presence of enhanced electromagnetic field at an interparticle junction on the long axis of the dimer of gold nanospheres.

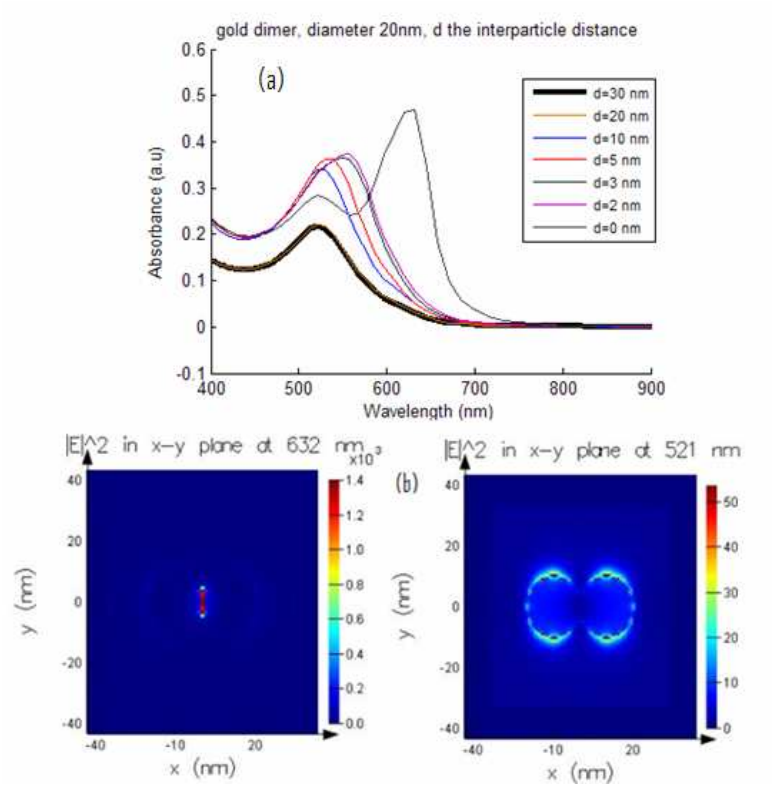

Figure 3. (a) FDTD calculated spectra of two spheres (diameter 20nm), where d is the distance between the spheres. As the particles are brought together until they are touching (d=0), the plasmon resonance peak shifts red. (b) Electric field near the dimer calculated by the FDTD model at the resonances 632 and 521nm for the particle close together. Note the incident light is propagating along the z-axis and is polarized along the x-axis (left) and along y-axis (right).

3.2 Gold nanorod

For our calculations, the nanorod is modeled as a cylinder which ends are capped by half spheres, the aspect ratio is defined as the ratio between its length and diameter. The layer of 5nm of CTAB is wrapped around a longitudinal face of the gold nanorod while the mPEG polymer sticks at both ends of the rod. First we study the nanorod of 55nm length and 24nm diameter. For CTAB we consider a value of 1.41 for its refractive index and 1.42 for mPEG. The presence of these polymers on the surface of gold nanorods plays on their optical properties. As the aspect ratio increases, the intensity of the absorption coefficient increases due to the larger degree of anisotropy of the particle. The results show a linear increase in the maximum of the longitudinal Plasmon resonance intensity and wavelength as the aspect ratio is increased in Figure 4. The transverse Plasmon is not presented here, as it is insensitive to the aspect ratio with fixed diameter.

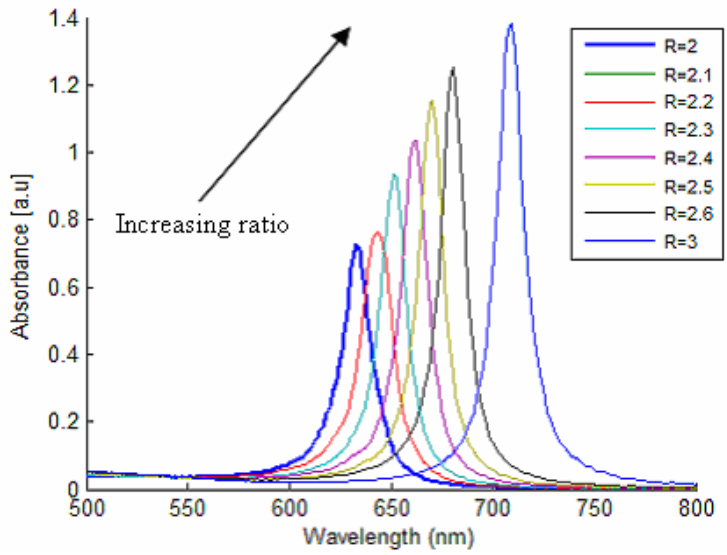

Figure 4. Longitudinal plasmon resonance absorption of single gold nanorod with diameter 24nm, coated with 5nm thickness of CTAB, calculated for different aspect ratios using FDTD simulations with 1.5nm grid resolution and incident light polarization along the major axis of the nanorod.

Figure 5 represents the near field on the rod excited with a field propagated along z-axis and polarized along the long x-axis of the rod at 646nm. One can see a collective oscillation of the charges along the long axis of the rod. This great field enhancement is important in the development of diagnostics tools. Nanorods are observed to have higher SERS signals than spheres, due to the higher electric field generated at the tips of the nanorod.

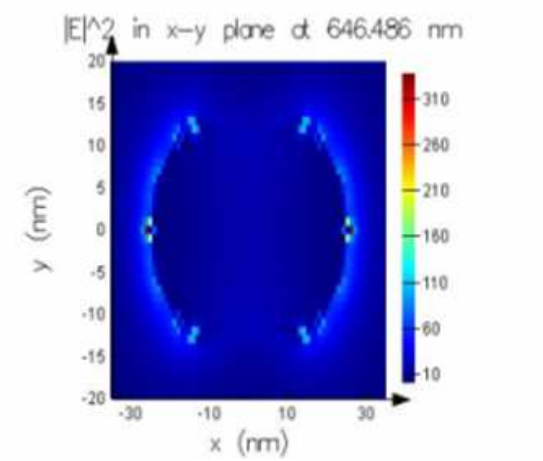

Figure 5. Electric field enhancement near the rod coated in CTAB, The incident light is propagating along the z-axis and is polarized along the x-axis.

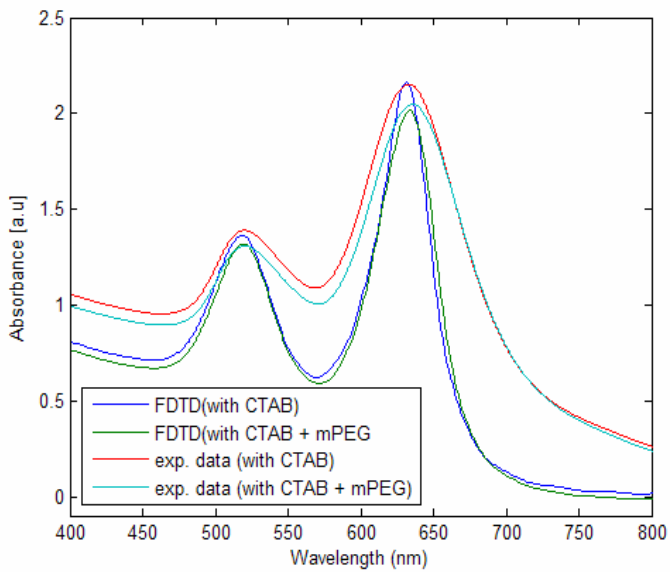

Figure 6. Absorption spectra of gold nanorods with 2.2 aspect ratio (L=53 nm, D=24 nm). From the top, the first and the second (red and turquoise) curves represent the experimental spectra of gold nanorods embedded in CTAB, and of nanorods conjugated with mPEG-SH respectively. The third and the fourth (blue and green) spectra are the FDTD corresponding simulations. We model the CTAB as 5 nm layer with n=1.41 refractive index around the longitudinal face of the rod. The mPEG is modeled by a 2 nm thickness half spherical outer layer, having n=1.42 refractive index around the half sphere situated at the end of the rod. λ_{T1}= 519.6 nm and λ_{T2}= 520.8 nm λ_{L1}= 632.6 nm and λ_{L2}= 635.4 nm

Figure 6 represents the results of our calculations compared with the experimental data. The calculations are done for a single nanorod with 2.2 aspect ratio. This result proves that the maximum contribution is referred to this ratio and that the mPEG has a slight effect on the position of the plasmon resonances. Moreover, the methoxy (polyethylene glycol)-thiol (mPEG) can be used to overcome the cytotoxicity caused by the presence of residual cetyltrimethyl ammonium bromide (CTAB), a surfactant required for nanorod synthesis and stabilization.

3.3 Silver nanoprism

In this section, we calculate with FDTD the optical properties of regular triangular silver prisms in water. We consider a diverse set of prisms to cover the range of possible excitations for this structure. It was noted that the full orientation could be approximated using three orientations [16], but orientations where the polarization vector E is parallel to the triangular cross section are most important to the overall extinction, while orientations where the polarization vector is perpendicular to the plane contribute much less.

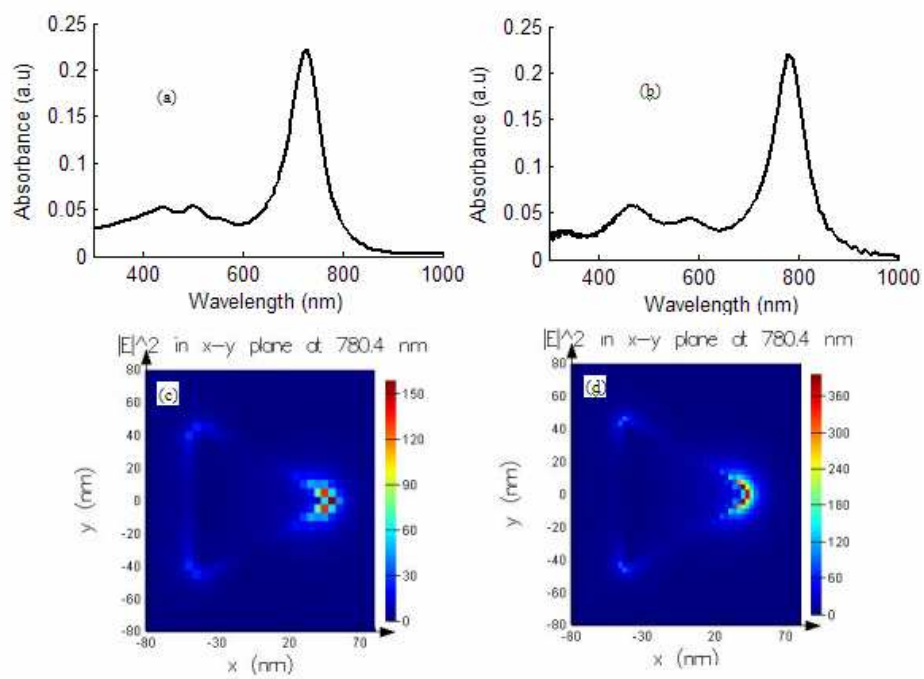

Figure 7. Absorption spectra of a triangular silver nanoprism in water solution.(a) edge length of 100nm and thickness of 20nm, (b) edge length of 100nm and thickness of 15nm, (c) corresponding electric field enhancement at 781.4nm, (d) corresponding electric field enhancement at 781.4 nm. In every case the incident light is propagating along the z-axis and is polarized along the x direction.

We see in these figures 7a and 7b that for each particle there are three dominant peaks in the absorbance spectrum, corresponding to different modes of plasmon excitation. In Figure 7a, we have abroad resonance with two maxima at 441.2 and 503.8nm attributed to quadrupole excitation, and a peak at 727.2nm corresponding to in-plane dipolar excitation. In Figure7b we find that the most intense peak 781.4nm corresponds to in-plane dipolar excitation. Also, the middle resonance 467.2nm is associated with in-plane quadrupole excitation and the bluest resonance which is at 334.4nm refers to out-of-plane quadrupole excitation. The positions of plasmon resonances depend, among other parameters, on particle size, or more specifically on the ratio between lateral dimensions and thickness (aspect ratio). Calculations indicate that the extinction spectrum of the nanoprisms is also sensitive to the thickness of the particles. For increasing the prism aspect ratio for fixed edge length, we note a red shift of the resonance corresponding to the dipole mode from 727.2 to 781.4nm. Figures 7c and 7d show the field enhancement for the two cases of nanoprisms we consider here, plotted as contours of $|E^2|$. One can see that the intensity of the near field is sensible to the prism aspect ratio. The anisotropic nanoparticles produce much stronger electric fields than that of the simpless structures as nanospheres, particularly for nanoparticles with sharp points such as triangular nanoprisms and branched nanocrystals.

4. Conclusion

In this work we calculate the optical properties of gold and silver nanoparticles of different shape and size. First we studied the gold sphere properties and the calculations are compared with the analytical existing results. The computed spectra agree very well with experimental results. The simulations showed a local electric field enhancement around the nanostructures, and in particular the nanoparticles assemblies show the largest field enhancement, confirming their utility in surface-enhancement Raman spectroscopy. We finish by theoretical calculations of the optical spectra of regular triangular silver prism and discuss their properties as function of edge length. The ability to provide large electric field enhancements make the triangular nanoprisms and branched nanostructures very attractive for applications in SERS.

Acknowledgments

The first author gratefully acknowledges the financial support from AUF (Agence Universitaire de la Francophone) project No CE/MC/466/08. Other authors gratefully acknowledge the financial support from CNCSIS project IDEI 477 /2007.

REFERENCES

1. Albert Polman, *Plasmonics Applied*, Science, 322, 2008, 868-869.
2. Andrea Alu and Nader Engheta, *Cloaking a sensor*, Phys Rev Lett. 102, 2009, 233901.
3. R. Elghanian., J. J. Storhoff, R. C. Mucic, R. L. Letsinger, C. A. Mirkin, *Selective Colorimetric Detection of Polynucleotides Based on the Distance-Dependent Optical Properties of Gold Nanoparticles* , Science, 277, 5329, 1997, 1078-1081.
4. S. Schultz, D. R. Smith, J. J. Mock, D. A. Schultz, *Single-target molecule detection with nonbleaching multicolor optical immunolabels*, Proc. Natl. Acad. Sci. U.S.A, 97, 3, 2000, 996-1001.
5. S.A. Maier, P. G. Kik, H. A. Atwater, S. Meltzer, E. Harel, B. E. Koel, A. A. G. Requicha, *Local Detection of Electromagnetic Energy Transport Below The Diffraction Limit in Metal Nanoparticle Plasmon Waveguides*, Nat. Mater, 2, 4, 2003, 229-232.
6. M. Baia, S. Astilean, T. Iliescu, *Raman and SERS investigations of pharmaceuticals*, Ed. Springer,2009.
7. G. Mie, Ann. Phys., 4, 25, 1908, 377.
8. J.P. Kottmann, O.J.F. Martin, D.R. Smith, S. Schultz**,** *Plasmon resonances of silver nanowires with a non-regular cross-section*, Phys. Rev. B, Vol. 64, Issue 23, 2001, pp.235402.1-10.
9. A. Taflove,S. C. Hagness, *Computational Electrodynamics:The finite-difference time domain method*, Artech. House, Inc., Norwood, MA, 2000.
10. D. M. Sullivan, *Electromagnetic Simulation Using the FDTD Method*, IEEE Press: Piscataway, NJ, 2000.
11. K. S. Yee, *Numerical solution of initial boundary value problems involving Maxwell's equations in isotropic media*, IEEE Trans. Antennas Propag., 14, 1966, 302-307.
12. R. J. Luebbers, F. Hunsberger, and K. S. Kunz, *A Frequency Dependent Time Domain Formulation for Transient Propagation in Plasma*, IEEE Trans. Antennas Propag, 39, 1991, 29-34.
13. R. X. Bian, R. C. Dunn, X. S. Xie and P. T. *Leung, Single molecule emission characteristics in near-field Microscopy*, Phys. Rev. Lett., 75, 1995, 4772-4775.
14. Lumerical (ID:4D3AB99E).
15. C. F. Bohren and D. R. Huffman, *Absorption and Scattering of Light by Small Particles*, Wiley, New York, 1983.
16. R. Jin, Y. Cao, C. A. Mirkin, K.L. Kelly, G.C. Schatz, and J.G. Zheng, *Photoinduced Conversion of Silver Nanospheres to Nanoprisms*, Science 294, 5548, 2001, 1901-1903.